227
4/29/69

777

ORNL-4390
UC-25 – Metals, Ceramics, and Materials

FUELS AND MATERIALS DEVELOPMENT PROGRAM

QUARTERLY PROGRESS REPORT FOR PERIOD

ENDING DECEMBER 31, 1968

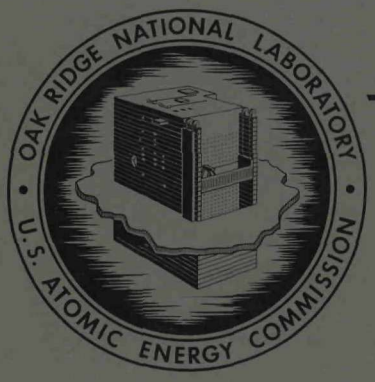

OAK RIDGE NATIONAL LABORATORY
operated by
UNION CARBIDE CORPORATION
for the
U.S. ATOMIC ENERGY COMMISSION

DISCLAIMER

Printed in the United States of America. Available from Clearinghouse for Federal
Scientific and Technical Information, National Bureau of Standards,
U.S. Department of Commerce, Springfield, Virginia 22151
Price: Printed Copy $3.00; Microfiche $0.65

5. ALKALI-METAL CORROSION STUDIES

W. O. Harms J. H. DeVan A. P. Litman

The purpose of this program is to investigate the chemical and metallurgical effects produced in structural materials during exposure to alkali metals. The program is designed to guide the selection of container materials for sodium-cooled fast breeder reactor systems and lithium-cooled space power reactor systems in which K serves as the Rankine-cycle working fluid. Forced circulation loop experiments of engineering scale are included in the test program.

Mass Transfer of Interstitial Impurities Between Vanadium Alloys and Sodium

Although vanadium alloys are highly resistant to dissolutive attack by Na, they are quite reactive with nonmetallic impurities in Na, particularly with C, N, and O. Accordingly, we are investigating the mechanisms by which vanadium alloys are attacked in Na at impurity levels typical of service conditions in a reactor. Our program is concerned with four basic aspects of the oxidation process for vanadium alloys in Na: (1) the partitioning of O between vanadium alloys and Na; (2) the effects of alloying additions of Cr and Zr on the diffusion coefficient of O in V; (3) the effects of Cr and Zr in V on the oxide formed and on the dissolution of the alloys in Na; and (4) the solubility of V in Na as affected by the presence of O in either metal. We are also examining the kinetics of the transfer of C and N between vanadium alloys and types 304 and 321 stainless steel in a sodium circuit.

Oxygen Effects on the Compatibility of Vanadium and Sodium (R. L. Klueh)

We previously reported[1] on oxygen uptake by vanadium specimens contained in vanadium capsules at 600 and 800°C. Similar tests were made

[1]R. L. Klueh, Fuels and Materials Development Program Quart. Progr. Rept. Sept. 30, 1968, ORNL-4350, pp. 87–91.

at 600°C with a vanadium specimen in capsules of Mo and type 304 stainless steel. We chose Mo because it is relatively inert to oxygen interaction, and stainless steel because of its interest for liquid-metal fast breeder reactor (LMFBR) applications.

Except for the capsule material, the experimental system and test procedure were the same as described earlier.[1] Table 5.1 shows the weight gained by vanadium specimens as a function of the amounts of Na_2O added to the Na before test. As in the case of the all-vanadium systems,[1] weight was gained in proportion to the amounts of Na_2O added to the Na. Unlike the all-vanadium systems, however, which had no reaction products, the specimens exposed to Na with high oxygen content in these later tests had a dark surface scale. The scale on those contained in molybdenum capsules were quite black, while those contained in stainless steel were dark gray.

These specimens have now been submitted for metallographic and chemical analyses, and we are attempting to determine the nature of the scales.

Table 5.1. Weight Changes of Vanadium Specimens Exposed To Sodium Containing Various Amounts of Na_2O at 600°C

Container Material	Initial Oxygen Content of Sodium[a] (ppm)	Specimen Weight Gain[b] (mg)
Molybdenum	50	1.3
	450	5.0
	1000	8.9
	1800	14.6
	4000	14.3
Type 304 Stainless Steel	50	0.5
	550	3.8
	1100	7.6
	2050	11.2
	4000	20.6

[a] Oxygen added as Na_2O.

[b] Specimen size: 1 × 1/2 × 0.065 in.

Deoxidation of Vanadium by Molten Lithium (J. H. DeVan)

We have been examining techniques for altering the oxygen content of V without affecting other chemical or metallurgical properties of the metal. The ability to adjust the oxygen content of V would facilitate our investigation of the role of O in the process of corrosion by Na.

Though the concentration of O can be increased above that in as-received V by heat treatment in an environment of low-pressure O, the reverse process is more difficult, as attested by the problem of manufacturing V with low oxygen content. However, a potential technique for deoxidizing V was suggested by the results of lithium capsule tests conducted by DiStefano[2] in which he evaluated the effect of interstitially dissolved O on the corrosion resistance of V in Li. His studies were carried out in 0.62-in.-OD × 0.030-in.-wall-thickness × 4.0-in.-long vanadium capsules, each of which contained a vanadium coupon submerged in 3 in. of Li. He found that V containing even as much as 2200 ppm dissolved O was completely resistant to attack by Li at 800°C. More significantly, however, the initial oxygen content of all vanadium specimens, which ranged from 400 to 2200 ppm before test, was reduced to about 100 ppm after test. The level of N in the V in some cases went up and in other cases remained unchanged.

Based on these results, we recently exposed a set of vanadium tubes, end caps, and specimens to molten Li to provide low-oxygen vanadium capsules for our proposed sodium corrosion tests. The cross sections of the vanadium components ranged from 0.049 to 0.060 in. The reaction vessel used for the treatment was constructed from 2.5-in.-OD Nb–1% Zr tubing and is pictured with the vanadium components in Fig. 5.1. To augment the gettering capability of the Li and to counteract the possibility of N being picked up by the V, we also incorporated a coil of zirconium foil around the vanadium components. The vessel was filled with 280 g of filtered Li and heated for 100 hr at 800°C. The Li was then discharged from the vessel, and residual Li was removed by flowing liquid ammonia through the inlet and outlet lines to the vessel until no color change

[2]J. R. DiStefano, Corrosion of Refractory Metals by Lithium, ORNL-3551 (April 1966), pp. 68–69.

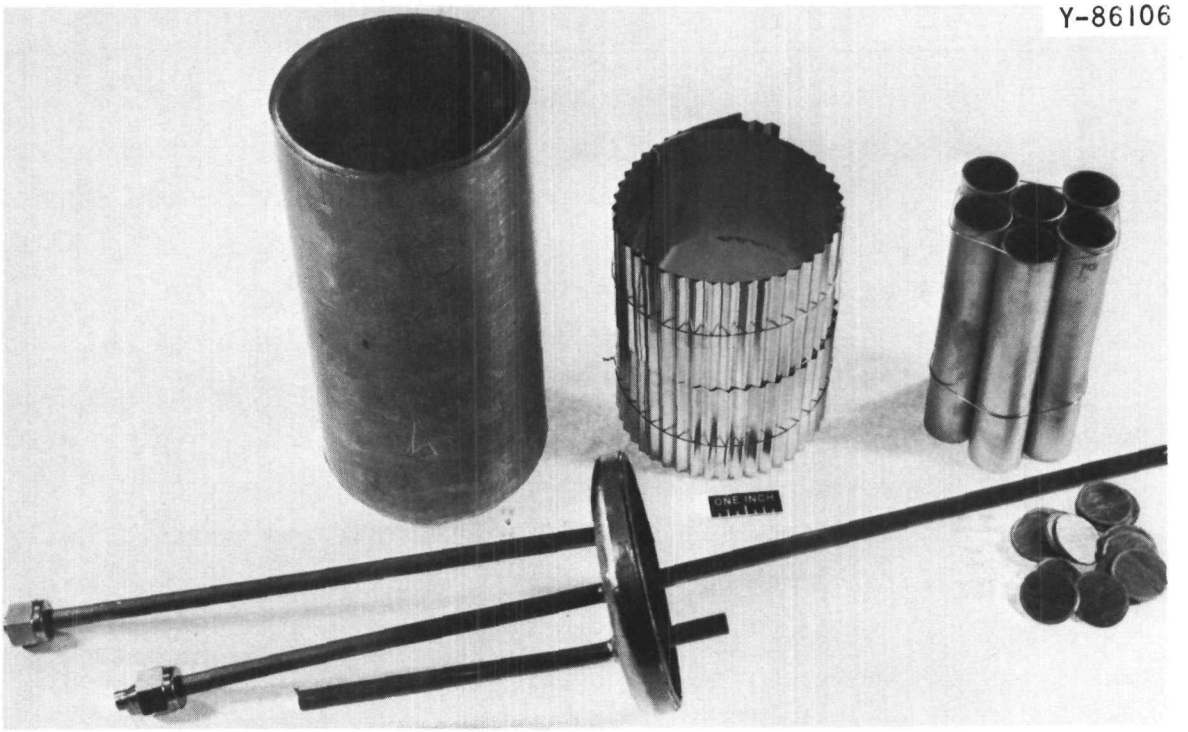

Fig. 5.1. The Nb–1% Zr Reaction Vessel (Left) Used to Lithium-Treat Vanadium Capsule Components (Right). Corrugated zirconium foil (center) was placed against vessel wall, surrounding vanadium components.

could be detected in the ammonia. The vessel was then opened, and the Li, the vanadium components, and the zirconium getter strip were chemically analyzed. The analytical results for the V appear in Table 5.2. In the case of the vanadium tubes, the analyses reflect the results of samples taken from each end and the middle of one tube. The oxygen level of all vanadium components decreased to below 100 ppm. The zirconium foil gained O roughly commensurate with the amount of O lost by the V. The nitrogen level of the V increased slightly despite the presence of zirconium foil. No chemical differences were detected among samples taken from different longitudinal positions on the vanadium tube. However, removal of 5- and 10-mil layers from the inside and outside surfaces reduced both the oxygen and nitrogen levels (Table 5.2). No metallographic changes were noted in the V, and the metallic impurities (including Li) were the same in vanadium samples before and after test.

These results indicate that lithium treatment could be used to reduce the oxygen level of commercially produced V whenever cross sections

Table 5.2. Effect of Zirconium-Gettered Lithium on Interstitial Content of Vanadium Metal After 100 hr at 800°C

Condition of Metal	Interstitial Content, ppm			
	O	N	H	C
3/4-in.-OD × 0.05-in.-Wall-Thickness Tubing				
As received[a]	1470	580	6	200
Lithium treated[a]	87	850	<1	230
Lithium treated, 5 mils machined from outer and inner surfaces	65	610	<1	200
Lithium treated, 10 mils machined from outer and inner surfaces	69	600	<1	220
3/4-in.-diam × 0.06-in. End Caps				
As received	1600	320	<1	470
Lithium treated	90	430	<1	470

[a]Average of three analyses.

are conducive to diffusion of O out of the V in reasonable periods of time. We are now evaluating the effects of time, temperature, and oxygen content of the Li on the kinetics of vanadium deoxidation.

Interstitial Contamination Effects in Vanadium and Its Alloys
(R. L. Wagner)

Interstitial contaminants in vanadium alloys significantly affect their metallurgical and mechanical properties. We are now evaluating the effects of alloying elements on the nature and rate of interstitial contamination of the following vanadium alloys in terms of temperature and vacuum conditions: V–5% Cr, V–10% Cr, V–15% Cr, V–1.5% Zr, V–5% Zr, V–10% Zr, and V–20% Ti. Reference studies on unalloyed V were begun at 500 and 900°C. As shown in Table 5.3, a 1-hr anneal at 900°C at 10^{-7} torr did not change the interstitial chemistry, but after 100 hr there was evidence of some decarburization. After 100 hr at 3×10^{-6} torr, the C decreased 60 ppm and the O increased 150 ppm. No weight change was

Table 5.3. Effect of Vacuum Exposure on the Interstitial Content of Vanadium[a]

Condition	Time (hr)	Pressure (torr)	Interstitial Analyses, wt %			
			C	N	H	O
As received			0.032	0.053	0.0007	0.021
Tested at 500°C	300	5×10^{-8}	0.034	0.051	0.0003	0.025
Tested at 900°C	1	1×10^{-7}	0.032	0.052	0.0002	0.022
Tested at 900°C	100	2×10^{-7}	0.029	0.053	0.0001	0.024
Tested at 900°C	100	3×10^{-6}	0.026	0.054	0.0002	0.036

[a]0.007-in.-thick foil.

observed for any of the samples after annealing. Related experiments[3] using this same equipment have extablished the major gaseous impurities to be H_2, C, N_2, H_2O, and CO_2.

We are evaluating other temperature and vacuum conditions and the value of protective wrapping with Ta. A furnace with a temperature gradient from 350 to 900°C is being set up to allow us to test several samples simultaneously and to vary the composition of our vacuum atmosphere.

Compatibility of Stainless Steel and Insulation in LMFBR Systems

A. P. Litman

We are studying the compatibility of stainless steel and thermal insulation, with and without the presence of Na, to guide the selection of containment piping and insulation for the Fast Flux Test Facility (FFTF) and future LMFBR systems. A comprehensive study of the literature will be followed by testing of types 304, 316, and 321 stainless steel between 370 and 760°C in air and in inert gas in contact with insulations and Na.

[3]H. Inouye, Contamination of Refractory Metals by Residual Gases in Vacuums Below 10^{-6} Torr, ORNL-3674 (September 1964).

The Effect of Insulation on the Oxidation of Stainless Steel

(C. D. Bopp)

During this reporting period, we completed the assembly of our oxidation test apparatus, which is shown in Fig. 5.2. This apparatus will be used both for the first part of this study, which deals with compatibility of thermal insulation in contact with stainless steel, and for the second part of the program, which deals with the effect of a small leak on the corrosion of the system.

We are testing relatively large specimens, 3/4-in.-diam × 5-in. long tubes, to simulate more closely actual LMFBR container materials and to match the sensitivity of an available chromatograph. During oxidation, the O_2 consumed and the H_2 generated (in moist air) are measured with a gas chromatograph. A measure of the permeability of the insulation is obtained from the pressure drop across the manometer shown in Fig. 5.2. After test, the tube specimen is removed, weight changes are recorded before and after the scale is removed, and the specimen is metallographically examined.

The test arrangement used for our first experiment with type 316 stainless steel tube is shown in Fig. 5.3. Ceramic filler pieces will be used in future tests to reduce the volume of the oxidation tube and the moisture meter, but they were not available for this preliminary test. The degree of stagnation of the atmosphere produced by the insulation was therefore less than we would have liked (see Fig. 5.2), since stagnation may accelerate oxidation (i.e., produce catastropic oxidation) by confining either MoO_3 vapor from materials that contain Mo or volatile substances from certain types of insulation. After 300 hr at 800°C in dried air (passed over $CaSO_4$ at 25°C), the metal loss from a specimen after removal of the scale was 8 mg/cm^2, and the scaling did not appear to be any more severe on the portion of the tube in contact with Kaowool. This rate of scaling is of the same magnitude as that found by others[4] at 870°C. We are conducting a test at the same temperature, 800°C, in

---

[4]A. de S. Brasunas, J. T. Gow, and O. E. Harder, "Resistance of Iron-Nickel Chromium Alloys to Corrosion in Air at 1600–2200°F," pp. 129–152 in Symposium on Materials for Gas Turbines, Buffalo, New York, June 24–26, 1946, Philadelphia, 1946.

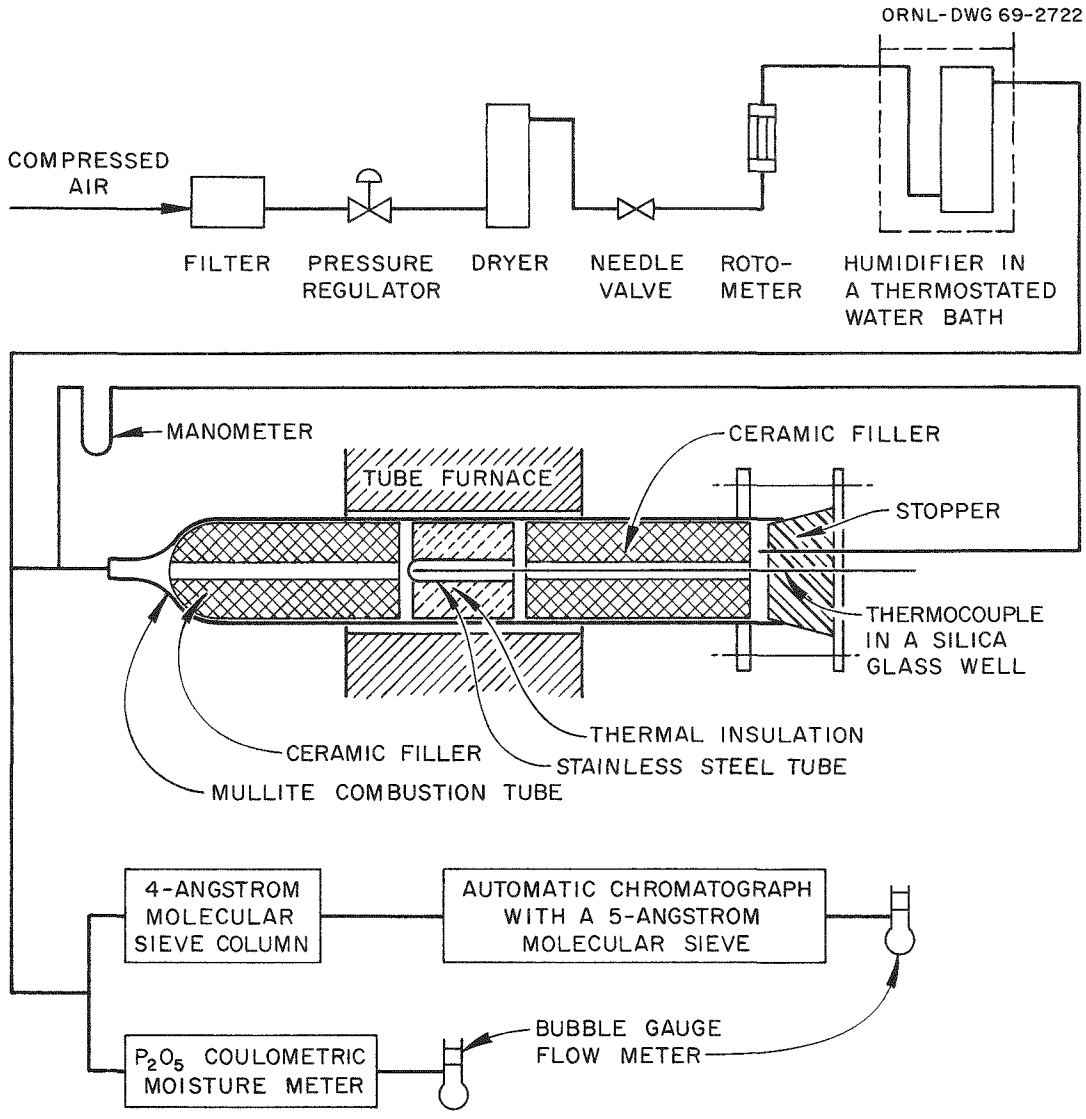

Fig. 5.2. Schematic Diagram of Apparatus for Insulation-Stainless Steel Compatibility Test.

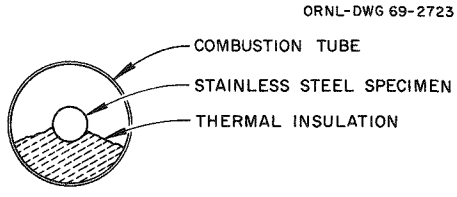

Fig. 5.3. Configuration for Preliminary Test of Interaction Between Stainless Steel and Thermal Insulation.

moist air (saturated with water vapor at 20°C), and the preliminary data for oxygen consumption indicate that the scaling rate is not much greater than in dry air.

Analysis of Mass Transfer Mechanisms in Loop Systems

R. B. Evans III

At the present stage of technology, mathematical treatments of mass transport in alkali metals stop short of considering solid-state diffusion effects. Since past studies at ORNL have underscored the importance of solid-state diffusion to mass transport at high temperatures, we are attempting to factor this added transport step into existing classical dissolution-deposition treatments.[5–7] The resultant equations are being compared against experimental findings for nickel- and iron-base systems operated with Na both at ORNL and at other laboratories.

In order to handle the rather complicated temperature profiles of these experimental systems, we have set up a computer program that allows us to divide the system into an arbitrary number of segments, across any one of which temperature can be assumed to vary linearly with distance along the loop.

There are several obstacles to acquiring a definitive treatment of existing experimental information, and these are worth noting for future experimental designs. The most serious difficulties stem from complicated geometry and temperature profiles, the uncertainty as to supersaturation effects, and the confusion about whether solute is carried in

---

[5]J. J. Keyes, Jr., Some Calculations of Diffusion Controlled Thermal Gradient Mass Transfer, ORNL-CF-57-7-115 (July 22, 1957).

[6]L. F. Epstein, "Static and Dynamic Corrosion and Mass Transfer in Liquid Metal Systems," Vol. 53, p. 67 in Liquid Metals Technology, Part 1, Chem. Engr. Progr. Symp. Ser. 20, American Institute of Chemical Engineers, New York, 1957.

[7]W. R. Grimes, G. M. Watson, J. H. DeVan, and R. B. Evans, "Radio-Tracer Techniques in the Study of Corrosion by Molten Fluorides," pp. 559–574 in Conference on the Use of Radioisotopes in the Physical Sciences and Industry, September 6–17, 1960 Proceedings Vol. III, International Atomic Energy Agency, Vienna, 1962.

part as particulate matter. Finally, in many systems there have not been enough determinations of weight change to yield a reliable measure of mass transport rates at every loop position.

In order to supplement the existing information on weight change for the several nickel alloy-sodium systems operated at ORNL,[8] we are submitting specimens from several loops for microprobe analysis. Concentration profiles of the alloy constituents in the loop walls and in crystalline deposits should shed considerable light on the mechanism involved and on the kind of mathematics one might use (even semiempirically) to describe corrosion rates in this particular system.

Corrosion of Refractory Alloys in Lithium, Potassium, and Sodium

J. H. DeVan A. P. Litman W. R. Huntley

Requirements for auxiliary electricity or ion propulsion for space vehicles necessitate power plants of high efficiency that will operate at high temperatures. For these applications, nuclear power systems have been proposed in which alkali metals are used to transfer heat, drive a turbogenerator, and lubricate rotating components. Accordingly, we are investigating the corrosion properties of candidate alkali metals, primarily Li and K, under conditions of interest for space applications. Because of the relatively high temperatures (>1000°C), the investigation is concerned largely with refractory-metal container materials.

Forced Circulation Boiling Potassium Loop Tests (FCL-8)
(C. W. Cunningham, B. Fleischer)

Loop FCL-8, constructed of the niobium alloy D-43, is the third and final test in a series of forced convection loops designed to evaluate the effects of boiling potassium and potassium vapor at high velocity on niobium-base alloys and on TZM alloy. The loop completed 10,000 hr of operation in June 1968, and metallurgical examination is in progress.

---

[8] J. H. DeVan, "Corrosion of Iron- and Nickel-Base Alloys in High-Temperature Sodium and NaK," pp. 643–659 in Alkali Metal Coolants (Proceedings of a Symposium, Vienna, 28 November – 2 December 1966), International Atomic Energy Agency, Vienna, 1967.

We have destructively examined the two-pass helical induction pump from loop FCL-8 to ascertain the reason for the drop in pump efficiency[9] encountered during test. Examination showed that the 2.2-in.-OD outer shell of the pump had expanded to produce a gap of 0.035 in. between the inner surface of this shell and the adjoining helix assembly. This allowed a considerable part of the K flowing through the pump to bypass the outer helix. The growth of this outer shell indicates that it operated at a much higher temperature than measured at the inlet and outlet pumps. The explanation for the higher temperature we now believe is associated with the unique economizer capability of the two-pass reentrant helical pump cell, which features two concentric helical flow passages separated by a single wall of Nb–1% Zr alloy. This configuration can act as a regenerative heat exchanger for the transfer of energy deposited in the pump cell by the drive motor during normal operation. Consequently, even though the pump inlet temperature was nominally about 595°C and the outlet temperature was about 720°C, our calculations show that the central portions of the pump cell wall could have exceeded 980°C. The creep rate of Nb–1% Zr at this temperature under the pressure load of the pump would be on the same order as that observed for the outer shell (1.6×10^{-6} hr^{-1}). Future pumps of this design must provide a temperature capability considerably above the proposed inlet-outlet temperature range.

Effect of Oxygen on Compatibility of Refractory Metals and Alkali Metals (R. L. Klueh)

Oxygen Effects in the Niobium-Potassium System. – In our studies to compare the effect of O in the different refractory metal-alkali metal systems,[10] we have completed further tests on the Nb-O-K system. Five capsules containing specimens of unoxidized Nb were exposed to K with several oxygen levels, and two capsules containing specimens of Nb with 580 and 1400 ppm O, respectively, were exposed to K with about 100 ppm O.

---

[9]B. Fleischer and C. W. Cunningham, Fuels and Materials Development Program Quart. Progr. Rept. June 30, 1968, ORNL-4330, pp. 91–93.

[10]R. L. Klueh, Fuels and Materials Development Program Quart. Progr. Rept. Sept. 30, 1968, ORNL-4350, p. 125.

All tests were conducted for 500 hr at 600°C by procedures described previously.[11] Results are shown in Table 5.4.

The surfaces of specimens exposed to K with high oxygen content appeared dull after test, but none of them appeared to have a scale. All specimens lost weight. The two specimens oxidized before test lost considerable O, while unoxidized specimens changed little in K with either high or low oxygen content.

Metallographic examination of the two oxidizied specimens indicated that they had been penetrated by the K. The penetration was much less severe than for similarly oxidized tantalum specimens exposed to K or for niobium specimens exposed to Na at 600°C. Since we believe penetration involves the formation of a compound containing O, the final concentration of O in the penetrated specimens may include O in the form of a corrosion product as well as O dissolved in Nb.

---

[11] R. L. Klueh, Fuels and Materials Development Program Quart. Progr. Rept. June 30, 1968, ORNL-4330, p. 142-146.

Table 5.4. Effect of Oxygen on Compatibility of Niobium and Potassium

Oxygen in Potassium Before Test[a] (ppm)	Oxygen in Niobium (ppm)		Weight Change[c] (mg)	Niobium in Potassium After Test (ppm)
	Before[b]	After[b]		
100	70	64	-0.2	960
530	70	68	-0.2	1060
1000	70	58	-1.1	2190
2030	70	57	-2.9	3380
3900	70	71	-7.0	3600
100	580	420[d]	-1.2	885
100	1400	520[d]	-5.5	1130

[a] Oxygen added as K_2O to K already containing about 100 ppm O.

[b] Determined by vacuum-fusion analysis.

[c] All specimens were about 1 × 1/2 × 0.04 in.

[d] Microstructures show that K penetrated these specimens.

Specimens with normal levels of O before test showed no significant metallographic changes. Microhardness profiles for these specimens indicated that the oxygen concentration was uniform across the specimen, and diffusion calculations confirmed that the oxygen concentration should have attained equilibrium across the specimen under our test conditions.

Partitioning of Oxygen Between Potassium and Zirconium and Between Sodium and Zirconium. — We demonstrated[12] that the equilibrium distribution coefficient for the partitioning of O between Zr and K or Na (atom fraction of O in Zr divided by atom fraction of O in alkali metal) is large enough to be considered infinite. Therefore, when Zr is exposed to the liquid metal, the amount of O originally present in the liquid, $C_O^{(A)}$, is given by

$$C_O^{(A)} = \Delta C_O^{(Zr)} \frac{W_{Zr}}{W_K} , \qquad (5.1)$$

where $\Delta C_O^{(Zr)}$ is the O gettered by the Zr and W_{Zr} and W_A are the weights of Zr and alkali metal, respectively.

We are evaluating the applicability of Eq. (5.1) for the analysis of O in K and Na. Our technique consists of exposing a given amount of alkali metal to a zirconium coupon in a molybdenum container for 100 hr at 815°C. After test, the capsules are inverted and quenched, the specimens are removed and cleaned in alcohol, and $\Delta C_O^{(Zr)}$ is determined by vacuum-fusion analysis. The technique has been referred to as a gettering-vacuum-fusion (GVF) analysis. Table 5.5 shows the results of evaluations of the K by the GVF technique; in these tests, known amounts of O were added to the K before test, and the amount of O recovered by the Zr was checked against the amount added. For oxygen concentrations up to about 1000 ppm, the amount recovered was within 10% of the amount added. At higher oxygen concentrations, however, the percentage recovered decreased significantly. Results of similar tests for Na are shown

[12] R. L. Klueh, Fuels and Materials Development Program Quart. Progr. Rept. Sept. 30, 1968, ORNL-4350, pp. 126–127.

Table 5.5. Oxygen Recovered from Potassium by Gettering-Vacuum-Fusion Analysis[a]

Total Oxygen[b] (ppm)	Oxygen Content in Zirconium (ppm)	Percent Oxygen Recovered by Zirconium
385	407	105
625	595	95
820	900	91
1125	800	71
1575	1000	64
2200	950	43
3000	1300	43

[a]All tests were made at 815°C for 100 hr on 0.04-in.-thick zirconium specimens.

[b]Initial O plus that added as K_2O.

in Table 5.6. In this case, the percentage recovered above about 1000 ppm O again decreased, but the decrease was not as large as for the tests with K.

We selected Mo as the container material because it is relatively resistant to oxidation in alkali metals. Indeed, for all tests with Na and for those tests in which the K contained low concentrations of O, there was no indication of any attack on the Mo. However, the surfaces

Table 5.6. Oxygen Recovered from Sodium by Gettering-Vacuum-Fusion Analysis[a]

Total Oxygen[b] (ppm)	Oxygen Content in Zirconium (ppm)	Percent Oxygen Recovered by Zirconium
500	465	93
900	845	94
1250	945	76
1900	1450	76
2100	1900	90

[a]All tests were made at 815°C for 100 hr on 0.04-in.-thick zirconium specimens.

[b]Initial O plus that added as Na_2O.

of the molybdenum end caps that had been in contact with K that had a high concentration of O ($\gtrsim$ 1000 ppm) appeared etched, and metallography showed them to be faceted.

Zirconium specimens that had contacted the alkali metals with low oxygen content appeared unaffected. But zirconium specimens that had contacted the K with high oxygen content had a dull metallic appearance as opposed to their highly polished appearance before test, and specimens that had contacted Na with high oxygen content were covered by a dark-gray nonadherent film. X-ray diffraction showed that surfaces that had contacted the K with high oxygen content contained Mo and an intermetallic compound, Mo_2Zr. Bulk analyses of these zirconium specimens, which contained less than 10 ppm Mo before test, confirmed the presence of Mo:

Concentration (ppm)	
Oxygen in Potassium Before Test	Molybdenum in Zirconium After Test
385	930
625	1580
820	1130
1125	3300
1575	4500
2200	5800
3000	4400

By contrast, the surfaces of Zr exposed to Na with high oxygen content showed ZrO_2 with no evidence of molybdenum transport.

Oxygen had previously been shown to increase the solubility of Mo in K.[13,14] These results apparently reflect this effect and, in turn, suggest that this increased solubility causes significant dissimilar-metal mass transfer of the Mo in the K. The Mo and Mo_2Zr on the

[13]R. E. Cleary, S. S. Blecherman, and J. E. Corliss, Solubility of Refractory Metals in Lithium and Potassium, TIM-850 (October 1965).

[14]E. M. Simmons and J. F. Lagedrost, "Mass Transfer of TZM Alloy by Potassium in Boiling-Refluxing Capsules," pp. 237–271 in AEC-NASA Liquid Metals Information Meeting held in Gatlinburg, Tennessee, April 21–23, 1965, CONF-650411, USAEC Division of Technical Information Extension, Oak Ridge, Tennessee.

zirconium surface apparently act as a barrier to the absorption of O, thereby causing a decrease in the percentage of O recovered at the higher oxygen concentrations.

This interpretation is strengthened by the results of tests with Na. Our own unpublished studies of the comparative oxidation of Nb and Ta in alkali metals suggest that O does not affect the solubility of refractory metals in Na to the same degree as in K. The decrease in the percentage of O recovered from Na that contained > 1000 ppm O appears to be connected with the ZrO_2 formed. Mackay[15] showed that the oxidation of Zr in Na is independent of oxygen concentration in the Na above about 3 ppm O. If Mackay's extrapolated rate constant is used to calculate the amount of O that can be gettered in 100 hr at 815°C, all of the O present should have been recovered even if a ZrO_2 scale formed. The decrease in the percentage recovered in the sodium tests may have resulted from the loss of some of the surface scale when the specimens were prepared for vacuum-fusion analysis.

Table 5.7 shows the results of GVF analyses on K and Na that contained < 100 ppm O. A correction, which will be discussed in a future report, was required to account for O contributed by the Mo of the container. Also shown are results obtained by amalgamation. The two methods of determination agree quite well at these low levels of oxygen content. The concentration of Mo in the Zr did not change (< 10 ppm Mo both before and after exposure).

Corrosion of Refractory Alloys by Lithium

Thermal Convection Loop Tests (J. H. DeVan). — We are continuing our analysis of thermal convection loop TCL-6R, which operated with Li for 3000 hr with a maximum temperature of 1350°C in the hot leg. The loop was constructed of the tantalum alloy T-222 and contained T-222 insert specimens. Initial results[16] showed weight losses over two-thirds

---

[15]T. L. Mackay, Oxidation of Zirconium and Zirconium Alloys in Liquid Sodium, NAA-SR-6674 (February 1962).

[16]J. H. DeVan, Fuels and Materials Development Program Quart. Progr. Rept. Sept. 30, 1968, ORNL-4350, pp. 127–130.

Table 5.7. Comparison of Gettering-Vacuum-Fusion (GVF) and Mercury Amalgamation Techniques for Analysis of Oxygen in Potassium and Sodium

	Oxygen Concentration (ppm)	
	GVF	Mercury Amalgamation
Potassium	70	46
	88	52
	23[a]	28
	31[a]	35
	29[a]	28
	35[a]	43
	30[a]	30
	26[a]	31
Sodium	55	53
	41	35

[a]Potassium purified by vacuum distillation.

of the loop surface and locally high weight gains over the remainder. The weight changes correlated closely with the pattern of the migration of Hf around the loop.

We examined the concentrations of the interstitial impurities in insert specimens and tubing sections after their contact with Li in a thermal gradient. These chemical analyses are presented in Fig. 5.4. Tubing from the heater section of the loop showed a large increase in O. In contrast, tubing specimens from all other regions contained about the same O as before test, and the insert specimens lost O at all positions. Metallographic examination, as discussed below, indicated that the source of the O that contaminated the heater section of the tubing was external rather than associated with the Li.

We have observed a similar contamination problem in other experiments which, like this loop, were radiantly heated by an unalloyed tantalum heating element. Areas directly under the heater in each case were high in O while areas immediately away from the heater, which saw the same internal environment and temperature, were totally unaffected. It is significant that O was picked up even though the system pressure, as measured by a nude ion gage near the loop, was consistently in the

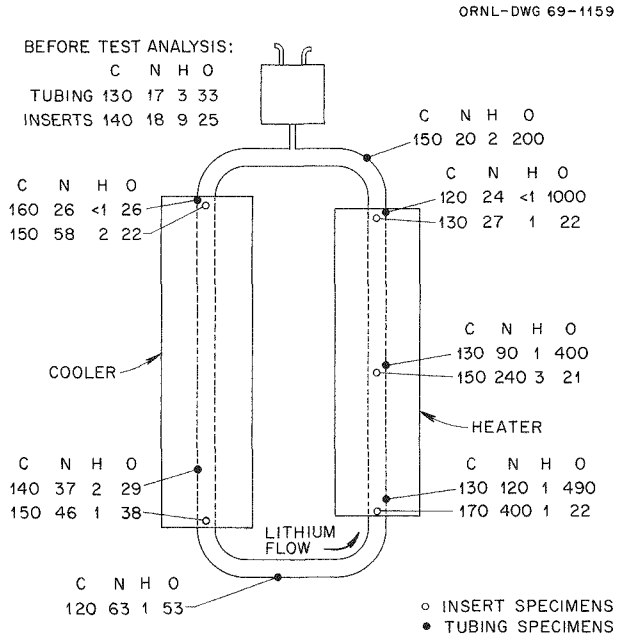

Fig. 5.4. Interstitial Content (ppm) of T-222 Loop Specimens After 3000-hr Test in Flowing Lithium at 1350°C.

range 10^{-8} to 10^{-9} torr. Judging from related test experience,[17] we believe we can circumvent the problem by substituting a tungsten-mesh heater element for the present tantalum assembly.

The nitrogen concentration in tubing and insert specimens increased in the colder regions of the loop and remained essentially unchanged in the hotter regions (Fig. 5.4). Point-to-point variations in carbon content were within the standard deviation of analyses for this element in T-222. The increase in N in colder regions of the loop ties in with the movement of Hf to these regions, as mentioned above, and also with the appearance in this region of a gold-colored film that has been identified by x-ray diffraction as HfN. Metallographic examination of specimens from colder regions revealed a relatively heavy concentration of an extremely fine precipitate evenly dispersed over the cross section of the specimen, as shown in Fig. 5.5(a). In the case of the hotter

[17] J. R. DiStefano, Refluxing Capsule Experiments with Refractory Metals in Boiling Alkali Metals, ORNL-4323 (January 1969), p. 25.

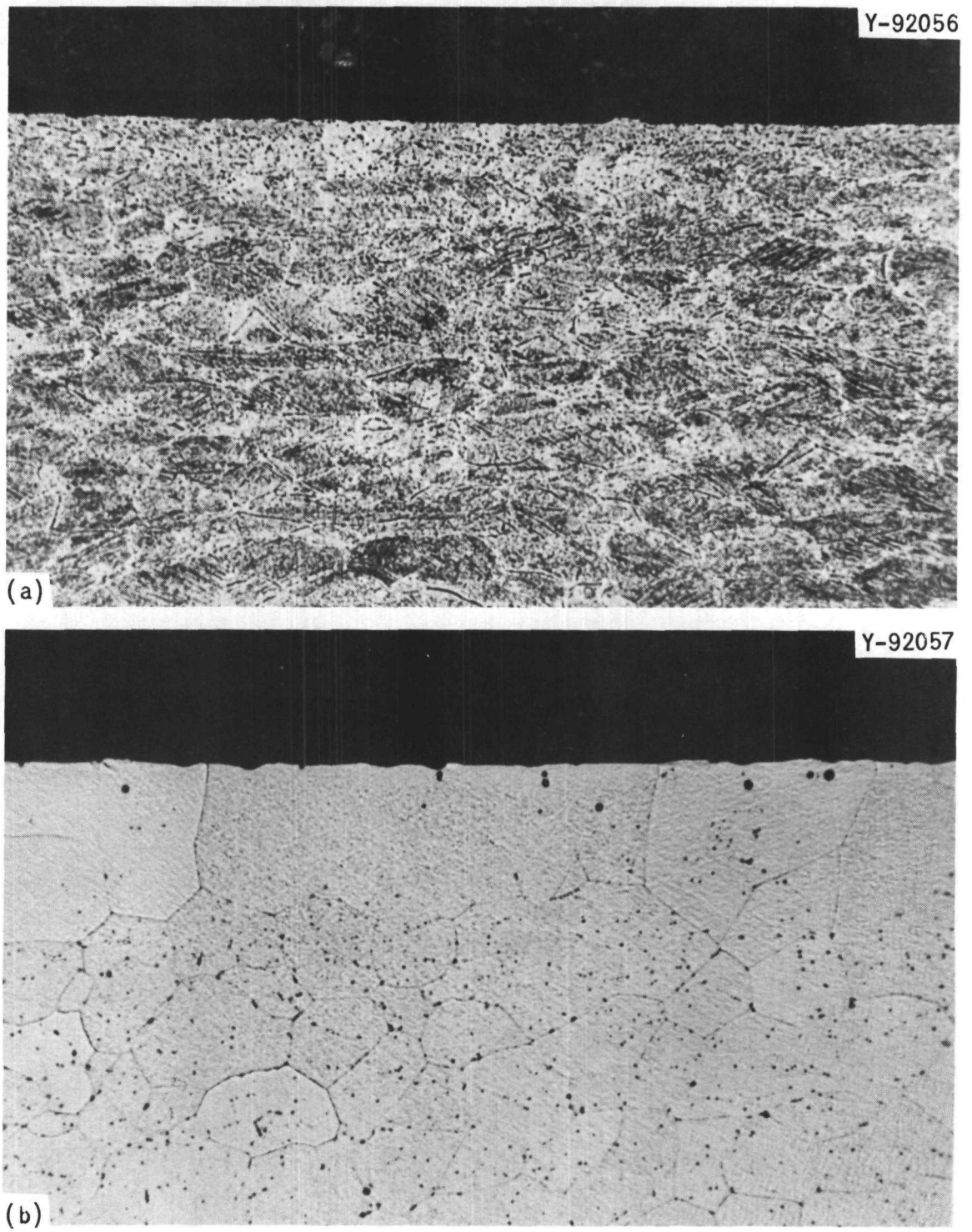

Fig. 5.5. Metallographic Appearance of T-222 Insert Specimens from Loop TCL-6R. Specimens were exposed to lithium for 3000 hr. 500×. (a) Minimum temperature position (1150°C) and (b) maximum temperature position (1350°C).

regions of the loop, we saw no metallographic changes in those insert specimens annealed (2 hr at 1600°C) before test [Fig. 5.5(b)]. Specimens that were partially cold worked were recrystallized during test but suffered no apparent effects of the exposure to Li.

The inside surfaces of tubing specimens appeared similar to the insert specimens, but external surfaces of tubing from the heater section showed evidence of internal oxidation to a depth of 17 mils and were covered by a very thin external layer that had the characteristics of a carbonitride film.

T-111 Forced Circulation Loop (FCLLL-1) (D. L. Clark, B. Fleischer)

We are constructing a T-111 forced circulation liquid lithium loop that will provide information on the corrosion of materials for cladding and containing fuel elements for lithium-cooled power systems for space. During this report period, we completed a leak check of the vacuum chamber for this facility and assembled the loop into the chamber.

Vacuum Test. — We made a trial evacuation of the vacuum chamber for FCLLL-1 to test the reconditioned triode ion pumps. The trial showed the pumps to be in good working order, and both a helium leak detector and a gas analyzer showed the chamber to be leak-tight against He. During subsequent bakeout, however, a large leak developed in the main flange after the chamber reached about 370°C. The flange was again leak-tight after the chamber had cooled to 80°C. In the future we plan to lower the rate of chamber heating to about 0.25°C/min so that leaks can be detected and eliminated, by tightening the flange, before they become excessive.

The auxiliary pumping system on the vacuum chamber was modified by the addition of a diffusion pump to the rough pumping system and by the installation of an optically baffled trap, cooled by liquid N, in the line between the auxiliary system and the chamber. This conversion makes it easier to detect leaks of He, decreases the likelihood of contaminating the system by back-diffusion of oil vapors, and shortens the period before the ion pumps can be activated. The base pressure attained by the rough pumping system was reduced from about 10^{-3} torr to 6×10^{-8} torr in 24 hr after starting at atmospheric pressure with a baked-out system backfilled with dry N.

Fabrication and Assembly of T-111 Loop Components. — After the annealing treatment,[18] the T-111 loop heater and economizer sections were welded, as shown in Fig. 5.6, and inlet and outlet lines were attached to the pump, as shown in Fig. 5.7. We welded transition joints of Nb–1% Zr and type 316 stainless steel to two lithium sampling lines attached near the pump inlet and outlet (Fig. 5.7) and welded a similar joint to the fill line entering the heater section (Fig. 5.6).

A leak check and penetrant inspection of these final assemblies revealed a leak where 1/16-in.-diam flowmeter wires had been tack welded

[18]B. Fleischer, Fuels and Materials Development Program Quart. Progr. Rept. Sept. 30, 1968, ORNL-4350, pp. 130–131.

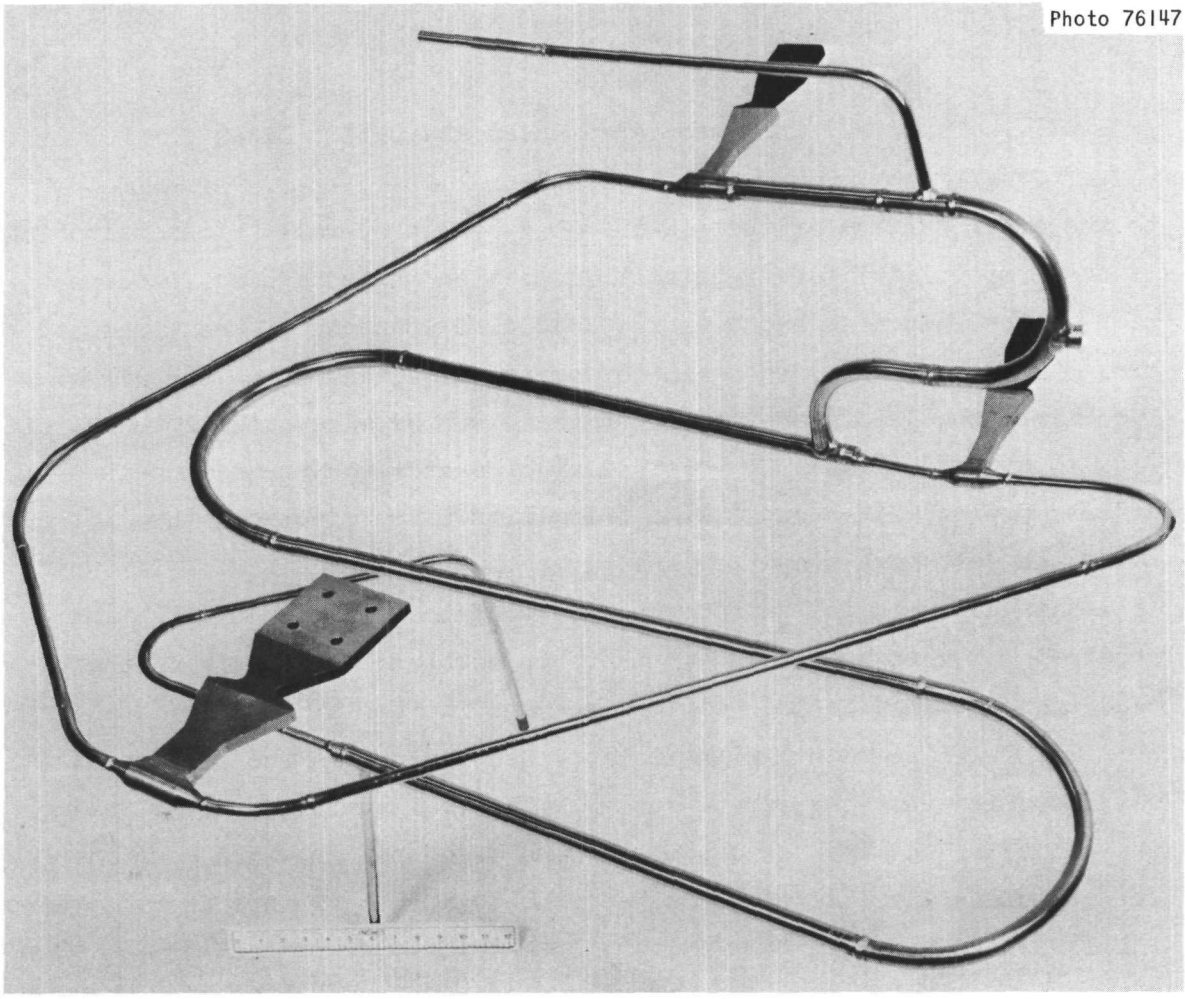

Fig. 5.6. Heater and Economizer Sections of FCLLL-1.

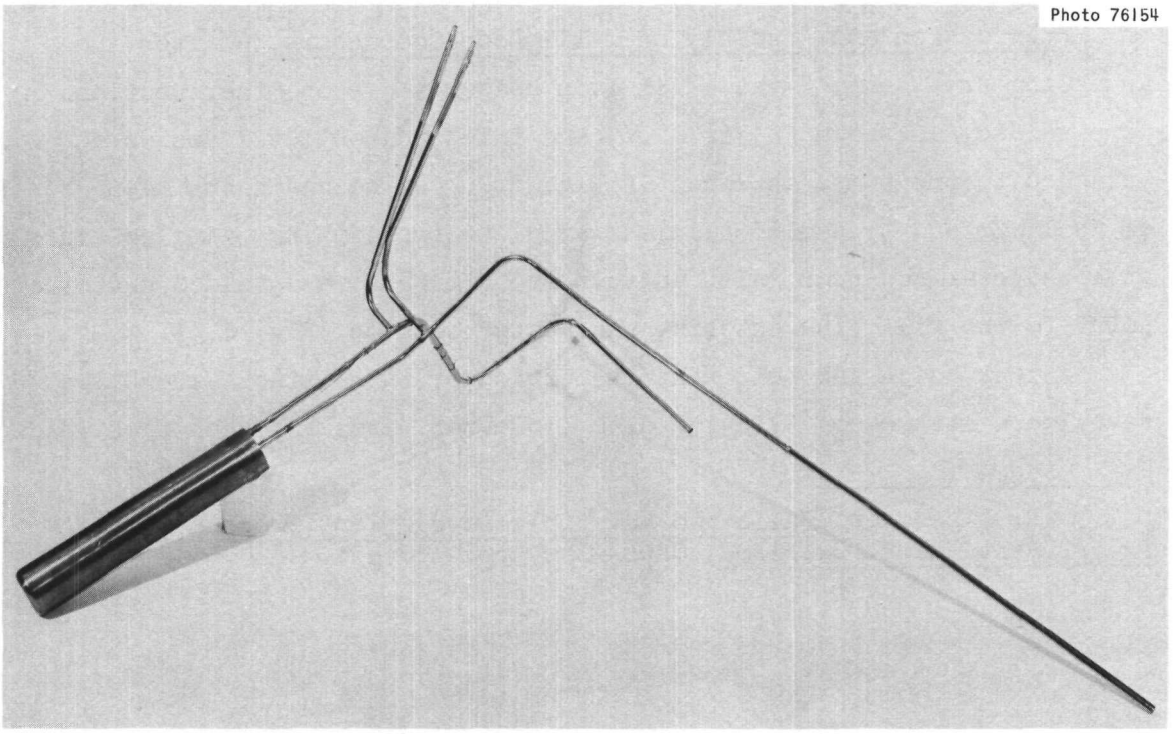

Fig. 5.7. Pump Cell and Associated Inlet and Outlet Lines for FCLLL-1.

to the outer surface of the 1/2-in.-OD × 0.065-in.-wall-thickness tubing of the pump inlet line. Penetrant inspection showed a crack under each tack weld. This area had been rewelded once when one of the wires had broken loose and rewelded again to correct misalignment of the wires. Each time, the welds were difficult to make. We alleviated both the difficulty of welding and the possibility of cracking by replacing the cracked piping with a machined fitting with tab projections that not only moved the weld area away from the piping but also made a self-fixturing, well-balanced weld design for attachment of the wires. This fitting required two more butt welds in the pump section. A picture of the redesigned section before welding is shown in Fig. 5.8.

The T-111 pump cell with its attached tubing was the first subassembly installed into the vacuum vessel. Type 321 stainless steel tubing was welded to the transition joints, and trace heaters were mounted on the stainless steel sections between the transition joints and the vacuum vessel penetrations.

The T-111 radiator section, pictured in Fig. 5.9, and the economizer and heater sections were next assembled on the test stand frame along with

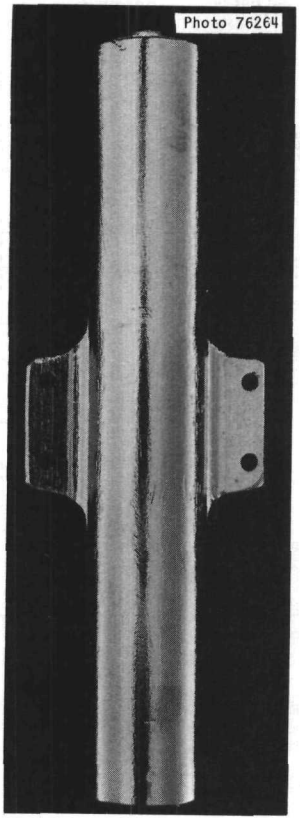

Fig. 5.8. T-111 Fitting for Attachment of Flowmeter Wires.

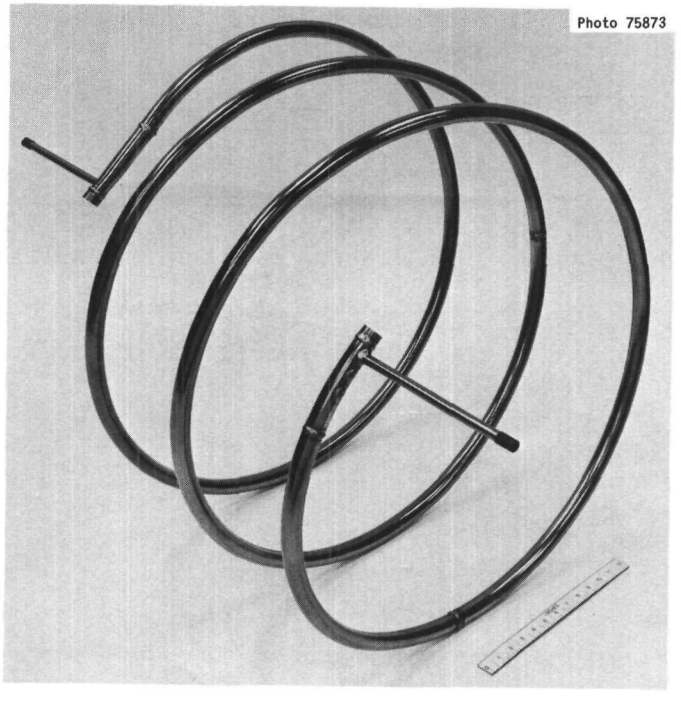

Fig. 5.9. Radiator Section of FCLLL-1.

the copper bus bar. Only one field bend was needed for proper alignment. The field weld between the economizer and radiator was made before the test stand frame was installed in the vacuum vessel.

Following installation of the test stand frame and T-111 sections, we completed the final fitup of the subassemblies and made the last two field welds. Figure 5.10 shows the assembly for the final field weld with the automatic welder in place.

Weld Corrosion Tests. — It is well known that contaminated welds in refractory alloys exhibit serious intergranular attack when exposed to Li. A solution to the problem is an anneal after welding. Accordingly, we have made corrosion tests for 100 hr at 816°C on weld samples made during the final assembly of the loop to determine if the atmosphere during welding was sufficiently free of contamination to eliminate the necessity of annealing these final welds. One field weld, cut out of the loop for testing, was exposed to Li in a stainless steel capsule, whereas all the other samples were tested in a Nb—1% Zr pot. Because of impurities in the Li used, welds tested in the Nb—1% Zr pot were found to be contaminated by N after their exposure. Despite this effect, neither these samples nor the field weld showed any evidence of intergranular corrosion. Therefore, we concluded that the welds were satisfactory and eliminated the annealing step.

Final Installation of Minor Components of Loop. — The flowmeter magnet assembly, copper bus bar, high-current electrical feedthrough, and flexible connectors for the high-current feedthrough were installed inside the vacuum vessel. All heaters and thermocouples were installed for the fill and drain tank, the sampling glove box was completed, and the units were coupled to the vacuum-vessel feedthrough.

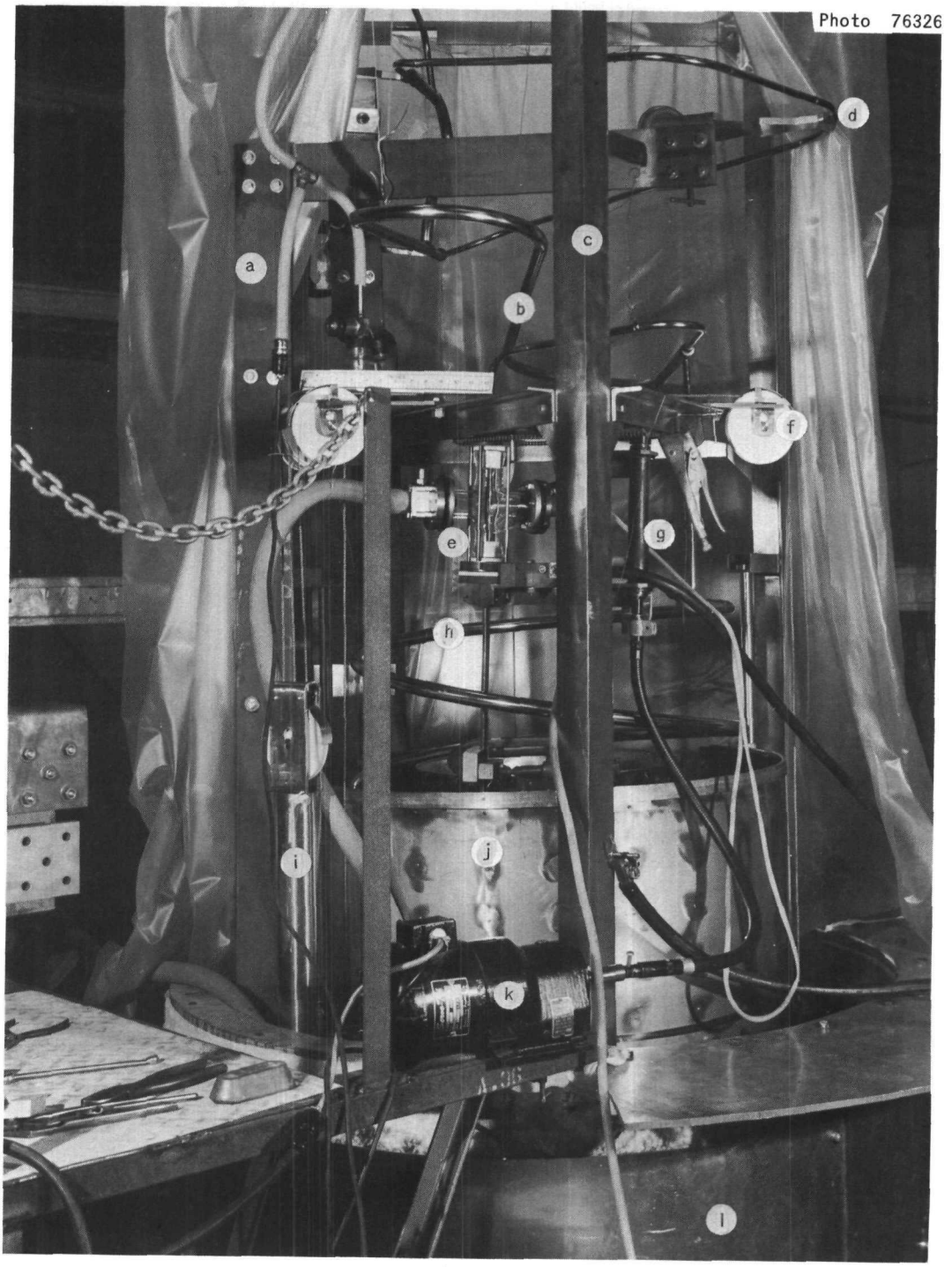

Fig. 5.10. Field Welding Assembly Used to Join Radiator and Economizer Sections After Installation of These Sections in the Vacuum Vessel. (a) Iron titanate coated copper bus, (b) economizer, (c) three-legged test stand frame, (d) resistance heated section, (e) Pyrex cross welding enclosure, (f) alumina sheave, (g) welding jig assembly, (h) radiator, (i) counterweight for shutter, (j) shutter assembly, (k) rotation drive unit, and (l) bottom part of vacuum vessel.